

# ZTF Starflat Observations

J. Nordin, M. Rigault, P. Rosnet

February 7, 2020

## Abstract

Starflats provide the most precise and accurate method to evaluate the pixel to pixel total system sensitivity. Any other method to evaluate this involves assumptions that can be challenged. To ensure that the ZTF photometry can be fully calibrated we here propose for the partnership to obtain one set of starflat dithers in each of the three filters during the Summer 2020 semester.

## 1 Scientific Justification

Starflats complement the measurement of spatial variations of CCD sensitivity obtained with the domeflat illuminator (called domeflats or high-frequency flats). Using individual stars as a probe, starflats map sensitivity variations at spatial scales larger than a few hundred pixels, where the light uniformity of the domeflat screen starts to degrade due to the discrete placing of the light sources (LEDs) in the illuminator. Using direct light, starflats make it possible also to examine and correct for effects, such as reflections, introduced by the diffuse nature of the light emitted by the illuminator.

By dithering the telescope pointing by many small angles around a field of moderate stellar density, the same star will be observed at different positions on the focal plane. As the observations spans less than a few hours the properties of the atmosphere can be assumed to be stable, and any change in the photometry of the objects is attributed to differences of camera sensitivity at different focal plane position.

Starflat dithers form a key component of the calibration pipelines of the photometric instruments that are currently considered state of the art: PS1 [Mag07], CFHT/SNLS [RCG+09] and DES [MGM+18]. These facilities typically repeat the starflat observations twice each year to monitor telescope and/or instrument aging. SDSS achieved a similar photometric quality, but through a combination of driftscan and uhercal (not possible on a fixed grid as used by ZTF).

### 1.1 Focal plane distribution of magnitude residuals

Figure 1 presents the distributions of the mean magnitude difference  $m_{diff}$  over the focal plane, derived from the relative count difference as the same star is reobserved, taken from the 2019 set of star flat observations (see Technical description). As visible there are three main types of features, all characterized by positive magnitude residuals (the ZTF magnitudes are larger than the PS1Cal ones), namely:

- Broad circular structures centered on each CCD.
- Small-scale blobs.
- CCD edges.

Since the starflat maps are obtained after domeflats are applied to the image, each of these features points to effects that are not corrected (or induced) by the high-frequency flats. When the magnitude residuals are positive (ZTF measure less flux than PS1) as in these cases, this indicates that the domeflats are over-estimating the pixel sensitivity.

A pipeline for processing starflat observations and producing a complete pixel sensitivity correction map was developed by M. Gojomi and provided to ZTF. This includes fitting a model to each Readout Channel which excludes small scale fluctuations and dust grain reflections. A sample model fit is shown in Fig. 2. From the residual map it is also clear that the model fails to reproduce

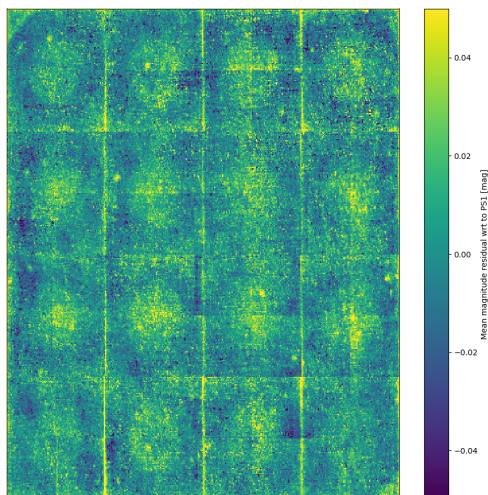


Figure 1: Distribution of  $m_{diff}$  as a function of position on the focal plane. To produce this plot, the magnitude residuals in each RC are binned in position. What is shown is the mean magnitude difference in each bin.

a large number of substantial small scale variations. In order to properly account for these small scale residuals, new dithered observations with a finer grid spacing are likely to be necessary.

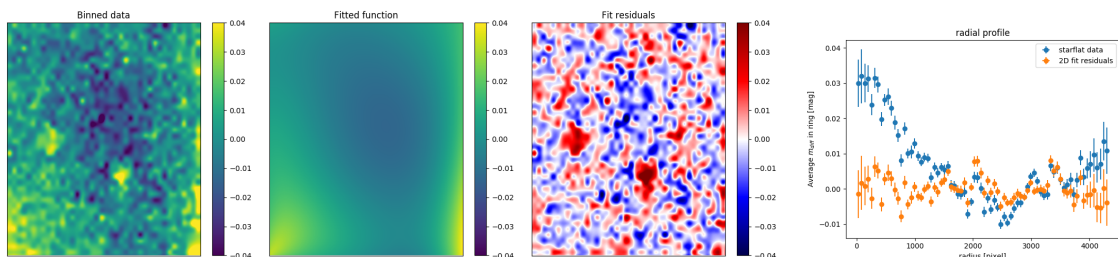


Figure 2: Fit results for the starflat map of RC 45 based on 2019 starflats. Left: distribution of magnitude residuals on the CCD quadrant. Left middle: fitted model, Right middle: 2D-Fit residuals. Note how the two large dust-grains are visible in the fit residuals, showing that the 2019 dither pattern was not sufficiently fine. Right: 1D

## 2 Current ZTF flatfield correction

The currently implemented IPAC processing pipeline makes use of the high-frequency dome flat corrections created each day, but no attempt at correcting for low-frequency variations are made. Andrew Drake has created a post-processing low-frequency correction map based on calibrator stars observed during normal operations. This contains many of the same qualitative features as the starflat map presented above, and the correction derived from this is provided as part of the alert packages.<sup>1</sup> Recently variations to these maps were also presented.<sup>2</sup> *The ZTF organization assumes these correlations to be sufficient and will thus not obtain any further on-sky starflat dither observations.*

We argue that starflat dithers are essential for demonstrating the accuracy of a complete photometric pipeline. Regular observation can be used to derive corrections, but are less well suited for testing the final data quality as they also rely on the details of e.g. atmospheric absorption, non-linearities, filter-bandpass and background estimate.

<sup>1</sup>Discussed in ZTF Newsletter 93

<sup>2</sup>ZTF Newsletter 112.

### 3 Technical description

#### 3.1 Proposal summary

It is in the interest of the ZTF partnership in general, and for groups that rely on accurate photometry in particular, to allow ZTF data to be calibrated at least to what is today considered a good standard. As this includes starflat observations we propose for the partnership to obtain one series of starflat dithers in each of the  $g, r, i$  filters. The 2019 starflats used 38 dithers and were found to still leave intermediate frequency variations and we thus suggest this number to be increased to 60. The total time spent will thus equal roughly one hour per band. This will allow us to create a state-of-the-art sample of transient lightcurves that can survive into the LSST era.

#### 3.2 Previous ZTF starflat observations

Two sets of starflats were previously obtained: A first set of dedicated observations was acquired on Feb. 21, 2018 during commissioning using the  $g$  filter. In Feb. 2019, a subselection of 38 of the same fields has been observed again, this time in all the three ZTF bands ( $g, r, i$ ). The Feb. 2018 dataset contained 203 exposures arranged on two overlapping pointing grids. Both grids probe, in logarithmic steps, spatial scales from tens to a few thousand pixels. The difference between the grids is in the pattern used to define the pointings, a rectangular one for the first grid and an hexagonal one for the second. The smaller set of dithers of Feb. 2019 focus on sampling intermediate-scale sensitivity variations, from a few hundreds to  $\sim 1500$  pixels. The three pointing grids are presented in figure Fig.3.

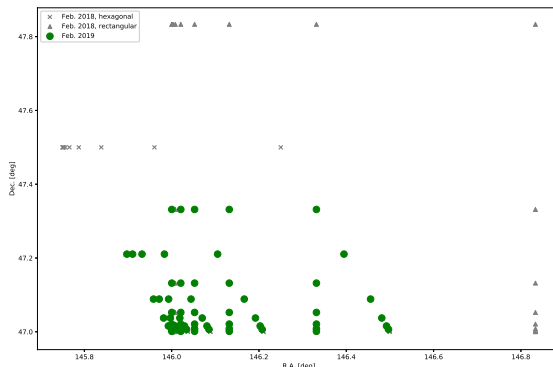


Figure 3: Telescope pointing positions used for the three starflat observations. The dithers used on Feb. 2019 are marked accordingly to the used pattern, rectangular (triangles) or hexagonal (crosses). The subsample of pointings observed in Feb. 2019 is highlighted in green.

#### 3.3 The proposed ZTF 2020 starflat observations

Each starflat sequence will be built from 60 closely separated dithers. These will be logarithmically spaced in both dimensions and the order scramble to further minimize effects due to changing weather conditions. The center location of these will be chosen as a region of intermediate star density with good visibility.

The starflats need to be taken during dark-time and photometric conditions, and all observations belonging to one filter should be taken sequentially. However, not all filters need to be observed during one night. We would also work with the schedulers to find a night which minimizes the impact to other programs. Such considerations could include choosing a night without a back-log of observations, no ToO requests, during P60/SEDm downtime or right after or before P48 service/down-time.

## References

- [Mag07] E. Magnier. *Calibration of the Pan-STARRS  $3\pi$  Survey*, volume 364 of *Astronomical Society of the Pacific Conference Series*, page 153. 2007.
- [MGM<sup>+</sup>18] E. Morganson, R. A. Gruendl, F. Menanteau, M. Carrasco Kind, Y. C. Chen, G. Daues, A. Drlica-Wagner, D. N. Friedel, M. Gower, M. W. G. Johnson, M. D. Johnson, R. Kessler, F. Paz-Chinchón, D. Petravick, C. Pond, B. Yanny, S. Allam, R. Armstrong, W. Barkhouse, K. Bechtol, A. Benoit-Lévy, G. M. Bernstein, E. Bertin, E. Buckley-Geer, R. Covarrubias, S. Desai, H. T. Diehl, D. A. Goldstein, D. Gruen, T. S. Li, H. Lin, J. Marriner, J. J. Mohr, E. Neilsen, C. C. Ngeow, K. Paech, E. S. Rykoff, M. Sako, I. Sevilla-Noarbe, E. Sheldon, F. Sobreira, D. L. Tucker, W. Wester, and DES Collaboration. The Dark Energy Survey Image Processing Pipeline. , 130(989):074501, Jul 2018.
- [RCG<sup>+</sup>09] N. Regnault, A. Conley, J. Guy, M. Sullivan, J. C. Cuillandre, P. Astier, C. Balland, S. Basa, R. G. Carlberg, D. Fouchez, D. Hardin, I. M. Hook, D. A. Howell, R. Pain, K. Perrett, and C. J. Pritchett. Photometric calibration of the Supernova Legacy Survey fields. , 506(2):999–1042, Nov 2009.